**CSIRO** PUBLISHING

# *Australian Journal of Physics*

Volume 52, 1999


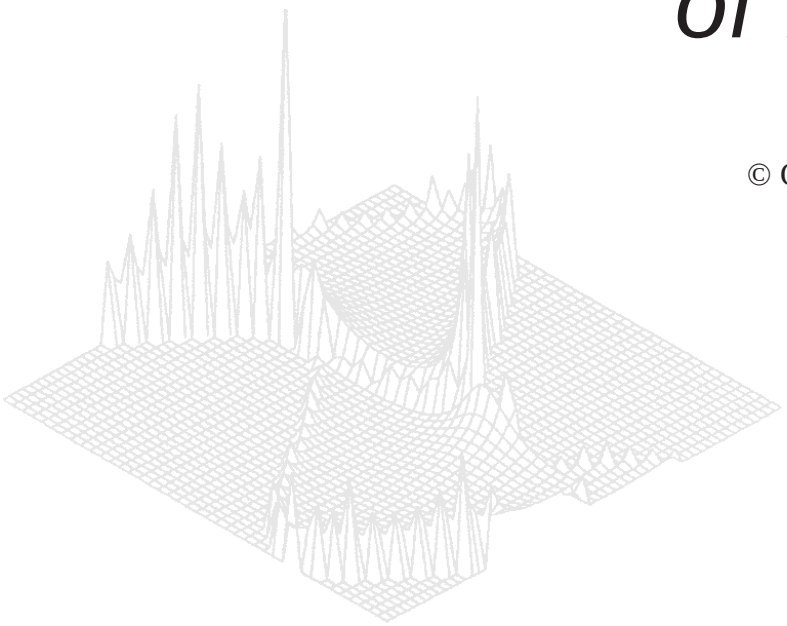

A journal for the publication of
original research in all branches of physics

**www.publish.csiro.au/journals/ajp**

All enquiries and manuscripts should be directed to
*Australian Journal of Physics*
**CSIRO** PUBLISHING
PO Box 1139 (150 Oxford St)
Collingwood Telephone: 61 3 9662 7626
Vic. 3066 Facsimile: 61 3 9662 7611
Australia Email: peter.robertson@publish.csiro.au

Published by **CSIRO** PUBLISHING
for CSIRO Australia and
the Australian Academy of Science

*Aust. J. Phys.*, 1999, **52**, 473–91

# Role of Negative Ion Resonances in Electron Scattering from Atoms and Molecules*

*S. J. Buckman, D. T. Alle, M. J. Brennan, P. D. Burrow,*[A] *J. C. Gibson, R. J. Gulley, M. Jacka,*[B] *D. S. Newman, A. R. P. Rau,*[C] *J. P. Sullivan and K. W. Trantham*[D]

Atomic and Molecular Physics Laboratories,
Research School of Physical Sciences and Engineering,
Australian National University, Canberra, ACT 0200, Australia.
[A]Department of Physics and Astronomy, University of Nebraska,
Lincoln, Nebraska, USA.
[B]Physics Department, York University, York, England.
[C]Department of Physics and Astronomy, Louisiana State University,
Baton Rouge, Louisiana, USA.
[D]Physics Department, Arkansas Technical University,
Russellville, Arkansas, USA.

*Abstract*

Transient negative ions (resonances) formed during the collision of an electron with an atom or molecule have been extensively studied for over thirty years. The continued interest in these states, both experimentally and theoretically, stems from the profound effects that they can have on electron scattering cross sections and the role that electron–electron correlations play in their formation and quasi-stability. A selective discussion of examples of such resonances, involving one, two and three excited electrons is given for a wide range of atomic and molecular systems.

## 1. Introduction

It is now well known that during low to intermediate energy electron collisions with atoms and molecules, the projectile electron can bind to the target atom or molecule for a short period of time to form a transient negative ion, or resonance. All atoms and molecules exhibit such resonances in varying degrees and, in some cases, the resonant enhancement of the scattering cross sections can be substantial. This is particularly true in the case of low energy electron scattering from molecules and, as a result, such processes have been of considerable interest to those communities that use such cross sections in the modelling of low temperature plasmas and gas discharges. Another, and more fundamental, reason for studying such systems is that the binding of the additional electron to the atom or molecule often involves a high degree of electron–electron correlation. In many cases the resonant state is a doubly (or triply) excited complex and, in order for the extra electron to cling to the neutral target, for times which can

* Refereed paper based on a contribution to the Australia–Germany Workshop on Electron Correlations held in Fremantle, Western Australia, on 1–6 October 1998.

 10.1071/PH99051 0004-9506/99/030473$10.00

be as long as $10^{-12}$ s, the two (or three) excited electrons must correlate their motion in order to share the smaller net positive charge of the ion core. As a result negative ion resonances have been viewed as a fertile field for the study of electron–electron correlation effects.

In this work, presented at the Australian–German Workshop on Electron Correlations, we shall review some of our recent activities in this area. In attempting to provide an indication of the importance of these states we shall consider examples from a number of different types of experiment, for a variety of atomic and molecular species. These will include:

- Studies of low energy (0–5 eV) electron scattering from diatomic molecules NO, CO, $N_2$ and $O_2$. The lifetimes of the low energy shape resonances supported by these molecules vary from $10^{-14}$ s to $10^{-12}$ s and the effects that they have on low energy scattering cross sections are profound.
- Recent measurements of triply excited, negative ion resonances in the autoionising region (57–62 eV) of helium. Measurements of the angular distributions of the electron which is autodetached in the decay of the 'hollow $He^-$' ions, as well as the branching ratios for their decay into excited states of the neutral atom, give some interesting insights into the nature of these highly excited states.
- Recent high resolution measurements of negative ion resonances in the Group II metals, Mg and Cd.

## 2. Experimental Techniques

A number of experimental techniques have been used over the years to study negative ion resonances, ranging from electron scattering, to laser photodetachment, to ion–atom scattering. A summary of these techniques is given in a recent review of the field by Buckman and Clark (1994). However, the overwhelming majority of work in this field has arisen from electron scattering studies and, as the lifetimes of these transient negative ion states are so short there is, to our knowledge, no technique which presently enables their efficient study in their own temporal domain. Rather, it is usual to study these transient states by monitoring the way in which they manifest themselves in electron scattering cross sections. They are formed in electron impact by the attachment of an electron to the target atom or molecule and they decay by autodetachment of this extra electron, either into the entrance channel (elastic electron scattering) or, if energetically favourable, into an excited state of the neutral atom or molecule (inelastic electron scattering). In the present work a range of varied experimental techniques, in our respective laboratories in Canberra and Lincoln, has been applied to the study of these states.

### *(2a) Time-of Flight Spectroscopy and Attenuation Techniques*

At very low energies, time-of-flight (ToF) electron spectroscopy has been used to measure the absolute total cross section for a number of diatomic molecules. If correctly applied at energies below 1 eV, the ToF technique can provide high energy resolution (<10 meV), high absolute energy accuracy (a few meV) and high accuracy (a few %) absolute cross section data. The apparatus used in the present studies is a linear transmission device which has been described in some

detail by Gulley *et al.* (1994) and Alle *et al.* (1996). Briefly it consists of a pulsed electron beam, formed by sweeping a high energy (∼200 eV), electrostatically collimated electron beam across a small aperture. The pulsed electron beam is retarded in energy and enters a 254 mm long scattering cell containing the gas of interest. Measurements of the transmitted electron current with both gas in $I_g$ and gas out $I_0$ of the cell, combined with a knowledge of the cell length $L$ and absolute gas number density $N$, are then used to obtain the total scattering cross section $\sigma_T$ with the Beer–Lambert attenuation law

$$\sigma_T = \frac{1}{NL}\ln\left(\frac{I_0}{I_g}\right).$$

This apparatus has been used to study the low energy (0·1–2 eV) total scattering cross sections for NO and $O_2$ and, in both cases, provides accurate absolute scattering cross sections and accurate absolute energies and widths for the wealth of low energy resonance structure associated with vibrational excitation of the lowest lying electronic states of $NO^-$ and $O_2{}^-$.

A similar type of experimental approach, which has been extensively used for resonance studies, is electron transmission spectroscopy (ETS, see Sanche and Schulz 1972). In these experiments resonance structure appearing in the total scattering cross section is detected with high sensitivity by measuring directly the derivative with respect to energy of the electron current transmitted through a vapour cell containing the gas of interest. The derivative technique serves to greatly enhance any sharp resonance structure with respect to the slowly varying background. The electron source is a trochoidal monochromator with energy resolution of approximately 35–40 meV. This apparatus has been used in the present work for studies of resonances in Group II metal vapours.

Whilst both of the above techniques provide accurate information about the energy and width of resonance structures and their role in the total scattering cross section, they are *not* scattering experiments and do not provide information about the nature of the the autodetached electron from which the resonance configuration can be obtained.

### *(2b) Crossed Beam Techniques*

There are distinct advantages arising from resonance measurements which include the detection of the energy and angle of the electron that is autodetached in the decay of the resonant state. In many cases this provides information about the final neutral atomic or molecular state involved in the decay and also the angular momentum that the scattered electron carries with it. Such information can then be used, together with simple arguments based on angular momentum and parity conservation and the nature of the entrance channel, to deduce the symmetry of the resonant state. Such measurements are usually carried out using a crossed electron–atom(molecule) beam geometry with a high resolution electron monochromator and energy analyser. For the measurements presented here three different crossed beam spectrometers have been used. The first is a conventional apparatus employing hemispherical energy analysers and electrostatic electron optics to produce a low energy (1–5 eV) electron beam of moderate energy resolution (30–50 meV) and intensity (1–5 nA). This apparatus is used to measure

absolute, differential electron scattering cross sections, employing the relative flow technique (Srivastava *et al.* 1975). It can also be used to measure absolute electron excitation functions where the energy dependence of an excitation cross section is determined with a view to revealing the role of resonances. This device has been described in detail (see for example Sun *et al.* 1995 and Gibson *et al.* 1996) and it has been used in the present work for excitation function measurements in $N_2$ and CO.

The second apparatus also uses a hemispherical energy selector in tandem with electrostatic electron optics to produce a high resolution electron beam (30–35 meV) which is crossed with a metal vapour beam effusing from a resistively heated oven. A range of detectors, including retarding potential analysers (RPA), photomultipliers and metastable atom detectors are used to monitor the energy dependence of a range of reaction products—elastic electrons, decay photons and metastable atoms—that arise from the electron collision. This apparatus has been used for studies of Group II atoms and it provides an interesting and useful complement to the results obtained from the Nebraska ETS apparatus.

The third crossed-beam apparatus also uses a hemisperical energy selector and analyser, although in this case the analyser has a large mean radius (15 cm) and is equipped with a position sensitive detector in its output plane which enables detection of scattered electrons over a broad energy range and greatly improves the efficiency with which data can be obtained. This apparatus has been described in a recent paper (Trantham *et al.* 1999) and we shall not repeat that detail here. In the work described here it has been used to measure the energy dependence of the differential cross sections for excitation of the four $n = 2$ levels of He, in the energy region of the doubly excited, autoionising states (57–60 eV) where a number of *triply* excited negative ion features have been previously observed.

## 3. Results and Discussion

### *(3a) Molecular Resonances*

#### $N_2$

The low energy shape resonance in molecular nitrogen has been studied in more detail than any other electron–molecule scattering system. This resonance, which occurs in the $^2\Pi_g$ symmetry, manifests itself as a series of dense, complicated oscillations in low energy elastic scattering and vibrational excitation cross sections for the ground electronic state of $N_2$. The overwhelming amount of interest in this state arose many years ago, principally as a result of the unusual behaviour that is observed when monitoring the decay of this resonance as a function of energy, scattering angle and final molecular state. The energies of the quasi-vibrational resonance features are observed to shift in differential scattering measurements, depending on both the final state being monitored and the angle of observation. This was first observed in a series of differential scattering experiments by Ehrhardt and Willmann (1967) and has been the subject of intense theoretical activity ever since. A summary of previous work is given in the recent papers of Sun *et al.* (1995), Weatherford and Temkin (1994) and Sweeney and Shyn (1997). This extensive theoretical activity led to the articulation of the 'boomerang model' (Herzenberg 1968). The lifetime of the resonance is similar to the vibrational

period of the negative ion ($\sim 10^{-14}$ s) and the intense, and varying energy oscillations in the cross sections result from interference between the outgoing and reflected nuclear wavefunctions. This model has been described in much detail by, for example, Birtwistle and Herzenberg (1971) and Schulz (1973).

Despite this activity, which served to pin down the *dynamics* of the resonance, there remained substantial discrepancies between experiments, and between experiment and theory, regarding the magnitude of the scattering cross sections in the region of the resonance. In part, and in hindsight, this appears to have been due to inappropriate comparisons being made between experiment and theory due to the difficulty in establishing meaningful points of comparison in the resonance region. It would appear that within this region the vibrationally elastic DCS at two energies separated by as little as 50 meV can differ appreciably, both in *shape* and *absolute magnitude*. Similar observations can be made with respect to the absolute magnitude of comparisons of vibrationally inelastic scattering. As almost all previous comparisons were made at *energies* specified by the various authors to correspond to resonance structures (peaks), a small energy uncertainty in any given work can lead to the possibility of large differences in the cross sections compared. In recent measurements and calculations of e–$N_2$ scattering, Sun *et al.* (1995) have adopted a protocol whereby comparisons are not made between experiment and theory at predetermined *energies* but rather at corresponding *structures* in the experimental and theoretical cross sections. Further detail on this technique can be found in Sun *et al.*

The results of this comparison are illustrated in Figs 1–3. Fig. 1*a* shows the absolute excitation function for elastic scattering in $N_2$ at a scattering angle of 60°, as measured on the ANU crossed-beam apparatus. The experimental results consist of data collected by scanning the incident electron energy at a fixed scattering angle and also individual points which arise from differential angular scans at a fixed energy. The two techniques show an excellent level of agreement

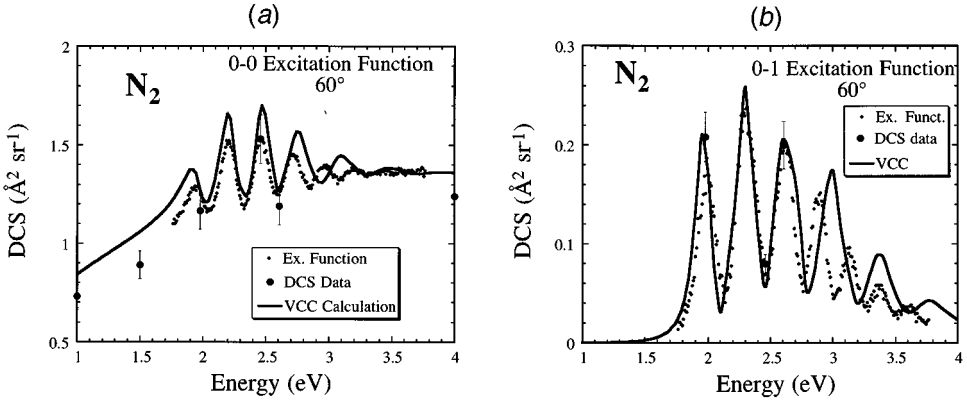


**Fig. 1.** Energy dependence of the absolute scattering cross section for (*a*) elastic scattering and (*b*) vibrational excitation of $N_2$ in the region of the $^2\Pi$ resonance, at a scattering angle of 60°. The small dots represent the excitation function measurement and the large solid points are the results of separate angular differential cross section measurements performed at a number of fixed energies. The curve is the vibrational close-coupling calculation of Morrison and co-workers. [From Sun *et al.* (1995).]

(typically within one standard deviation) across the shape resonance profile. Also shown is the energy dependence of the elastic cross section which was calculated by Morrison and co-workers, from the University of Oklahoma, using a vibrational close-coupling (VCC) approach. The agreement between experiment and theory, particularly at lower energies, is exceptionally good (within ∼10%). At higher energies the positions of the observed resonance peaks and those calculated differ substantially. In both cases the resonance contribution to the elastic cross section is about 30% of the non-resonant cross section. In Fig. 1*b* a similar plot is shown for the excitation of the first vibrational level of $N_2$. In this case the shape resonance clearly dominates the vibrational excitation process (in fact, as it is a homonuclear diatomic molecule there is *very little* direct vibrational excitation in $N_2$) and once again the comparison at low energies between experiment and theory is favourable. At higher energies the resonance structures are once again out of phase in experiment and theory.

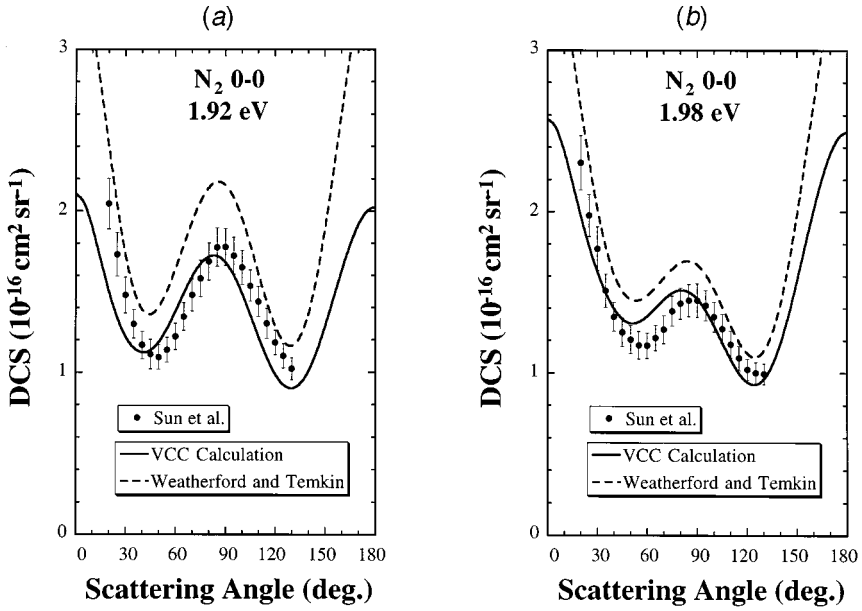


**Fig. 2.** Absolute DCS for elastic scattering from $N_2$ at energies corresponding to (*a*) the first peak in the elastic excitation function shown in Fig. 1*a* (1·92 eV) and (*b*) the first peak in the vibrational excitation function shown in Fig. 1*a* (1·98 eV).

In Figs 2*a* and 2*b* the differential elastic scattering cross section is shown at two energies which clearly illustrate the points made above regarding the need for a strict comparison protocol. Fig. 2*a*, at an incident energy of 1·92 eV, corresponds to the DCS at the position of the first resonance peak in the experimental *elastic* excitation function (see Fig. 1*a*), a structure which occurs at 1·90 eV in the theoretical calculation. Fig. 2*b* shows the corresponding DCS at an (experimental) energy of 1·98 eV, the energy of the first peak in the *vibrational* excitation function (see Fig. 1*b*), which occurs in the theory at 1·95 eV. A number of things are immediately obvious. Firstly, the shape of the two DCS are quite different, despite the energy difference between them of only 60 meV.

The expected d-wave character of the autodetached electron is clearly obvious in both cases, particularly the first which represents a measurement 'on-resonance' in the elastic channel. That the shape of the DCS is not a pure d-wave reflects the fact that there is also substantial non-resonant elastic scattering. In both cases the VCC calculation provides a good description of the DCS.

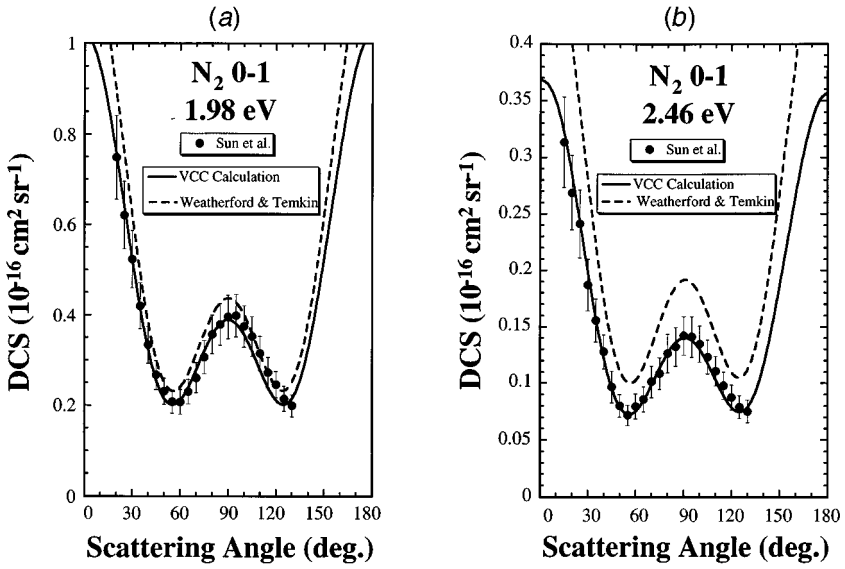


**Fig. 3.** Absolute DCS for vibrational (0–1) excitation of $N_2$ at energies corresponding to (*a*) the first peak in the vibrational excitation function shown in Fig. 1*b*—an energy of 1·98 eV—and (*b*) the second dip in the vibrational excitation function shown in Fig. 1*b*—an energy of 2·46 eV.

In Figs 3*a* and 3*b* we show examples of the DCS for vibrational (0–1) excitation of $N_2$. Fig. 3*a* is a measurement at 1·98 eV, corresponding to the first quasi-vibrational peak in the vibrational excitation function (Fig. 1*b*), whilst Fig. 3*b* is a measurement at 2·46 eV, an energy which corresponds to the position of the third peak in the elastic excitation function (Fig. 1*a*) and the second *dip* in the vibrational excitation function (Fig. 1*b*). With the exception of the different absolute magnitudes, corresponding to on- and off-resonance measurements, there is little difference in the two DCS. The shape of the cross section is essentially a pure d-wave character, indicating that vibrational excitation in this energy regime occurs almost entirely via the intermediate negative ion. The agreement between experiment and theory is excellent. A complete discussion of these results can be found in Sun *et al.* (1995).

*CO*

Low energy electron scattering from CO is also dominated by a shape resonance of $^2\Pi$ symmetry. CO is isoelectronic with $N_2$, has a closed shell structure but is weakly polar. Like $N_2$, this resonance has an intermediate lifetime such that it also exhibits quasi-vibrational structure (QVS) although, in this case, the structure is much weaker and superimposed upon a broad resonance envelope

between about 1·5 and 3 eV. As such it provides a formidable challenge for scattering theory in the low energy regime.

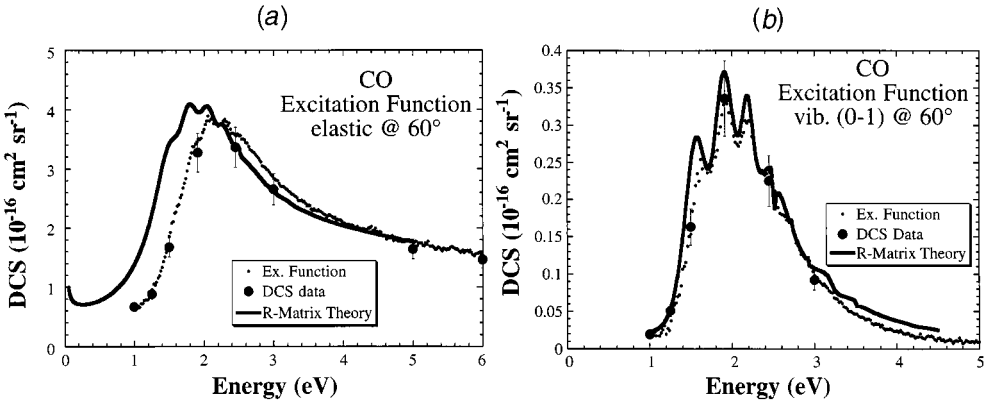


**Fig. 4.** Energy dependence of (*a*) the absolute elastic scattering cross section and (*b*) the first vibrational excitation mode at a scattering angle of 60°. Two experimental data sets are shown in each case: The small dots represent the excitation function measurement and the large solid points are the results of separate angular differential cross section measurements performed at a number of fixed energies. The solid curve is the R-matrix calculation of Morgan (1991).

This resonance structure is demonstrated in Figs 4*a* and 4*b* where we show excitation functions for elastic scattering and vibrational excitation (0–1) respectively. In Fig. 4*a* there is experimental evidence for the weak QVS at the peak of the broad resonance profile which also appears to be present in the *R*-matrix calculation (Morgan 1991; Morgan and Tennyson 1993). Indeed, with the exception of an energy offset of 200–300 meV, the theory and experiment are in excellent agreement. The QVS is much more evident in the vibrational excitation function (Fig. 4*b*) and the agreement between experiment and theory is very good. Once again the role of the resonance in providing vibrational excitation is clearly apparent, although in the case of CO, the small dipole moment (0·15 Debye) also provides a mechanism for direct vibrational excitation. A more extensive survey of these results is provided in Gibson *et al.* (1996).

### $O_2$

Molecular oxygen is an open shell molecule for which, until very recently, there were no high resolution, absolute cross section measurements at low energies. Such measurements are important as $O_2$, unlike $N_2$ and CO, supports a long series of well-established, vibrationally excited negative ion levels associated with the $^2\Pi_g$ ground electronic state of $O_2^-$. These vibrational levels manifest themselves clearly, and at definite energies, as the lifetime of the negative ion is of the order of $10^{-12}$ s, which is much longer than the vibrational period. As the first four vibrational levels $(0, 1, 2, 3)$ of the negative ion are bound the ground state of $O_2^-$ is stable and the electron affinity of $O_2$, which has been accurately measured in laser photodetachment studies (Celotta *et al.* 1972), is 0·440 eV. These resonances were first observed in differential electron scattering by Boness

and Schulz (1970) and Linder and Schmidt (1971), in the total cross section by Land and Raith (1973, 1974) and in recent times they have been the subject of a superb series of high resolution, differential scattering measurements by Allan (1995).

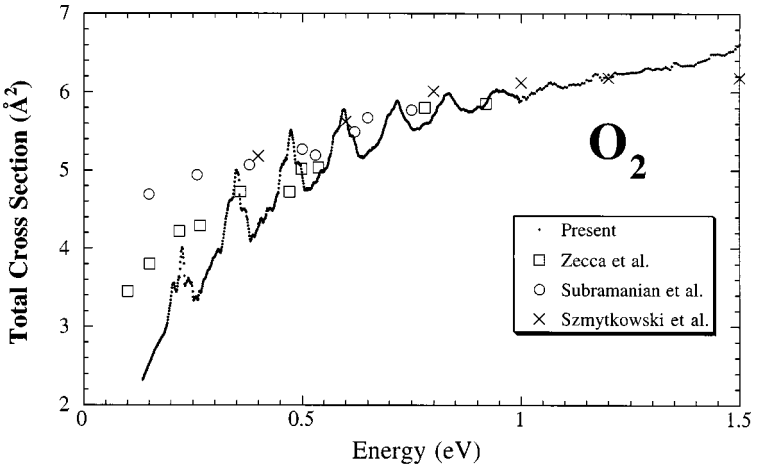


**Fig. 5.** Absolute total electron scattering cross section for $O_2$ indicating resonances associated with the vibrational levels of the ground state of $O_2^-$.

The present results pertain to the effect of these resonances on the absolute, total electron scattering cross section and they have been measured with the ToF electron spectrometer described briefly in Section 2. The total electron scattering cross section for $O_2$ at energies between 100 meV and 2 eV is shown in Fig. 5. A series of sharp vibrational resonances are clearly evident and these have a substantial effect (∼20%) on the total cross section at energies below 1 eV. A variety of other measurements of the total cross section are also shown (Zecca *et al.* 1986; Subramanian and Kumar 1990; Szmytkowski and Maciag 1996) and, whilst there is reasonable agreement as to the magnitude of the cross section between the present measurements and some of these, none of them illustrate the sharp resonance features seen in the present data. As a result of the ToF nature of the experiment and the high timing resolution achieved (∼500 ps), the energy scale of the present data is also quite accurate (±2 meV at 200 meV to ±12 meV at 800 meV). By determining the resonance positions we find vibrational constants for $O_2^-$ of

$$\omega_e = 135{\cdot}5 \text{ meV}, \qquad \omega_e x_e = 0{\cdot}875 \text{ meV},$$

and these values, together with the positions of the lowest observed resonance, result in a value for the electron affinity of 445±10 meV, in excellent accord with the laser photodetachment measurements. Further details of the experimental technique and analysis can be found in Alle (1999).

*NO*

Nitric oxide is yet another example of a diatomic molecule which possesses a relatively long-lived, low energy series of vibrational shape resonances. It is also a considerable challenge to scattering theory as it is both open shell and polar, with a dipole moment of 0·16 Debye. In addition, the ground ($^3\Sigma^-$) state of $NO^-$ is bound, with an electron affinity (EA) of a few tens of meV and it was the first such stable molecular negative ion whose EA was measured by laser photodetachment (Siegel *et al.* 1972).

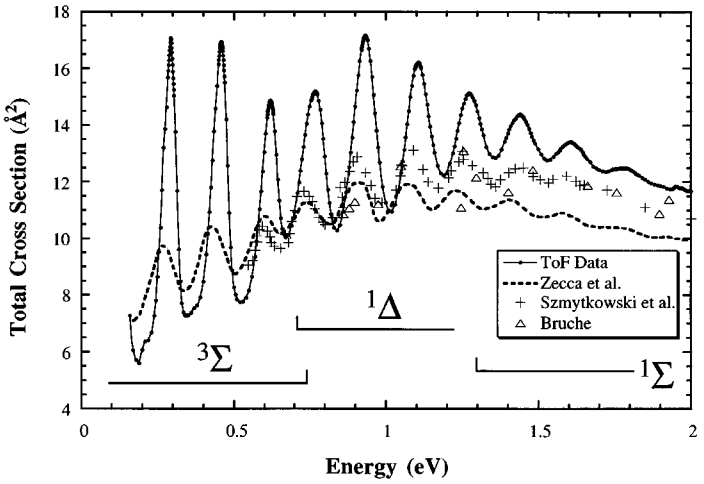


**Fig. 6.** Absolute total scattering cross section for NO. The strong resonance peaks are due to the formation of vibrationally excited $NO^-$ in the $^3\Sigma$, $^1\Delta$ and $^1\Sigma$ excited states, as indicated.

The low energy, total electron scattering cross section for NO has also been studied on the ToF spectrometer. This investigation, which measured the absolute cross section at energies between 0·1 and 5 eV with high energy resolution (∼15 meV) and high absolute accuracy of the energy scale (e.g. ±3 meV at 300 meV), yielded a remarkable series of resonance structures associated with the low lying $^3\Sigma^-$, $^1\Delta$, and $^1\Sigma^+$ electronic states of $NO^-$. These are illustrated in Fig. 6 where the dominant contribution of the resonances to the total cross section is clearly visible. Some previous experimental results with substantially lower resolution are also shown. The ranges of the three electronic states which lead to these vibrational structures are also indicated in the figure. The first three peaks of the spectrum correspond to the 0–2, 0–3 and 0–4 vibrational excitations of the $^3\Sigma^-$ ground state and they have an observed width of about 45 meV. The width of the fourth peak is substantially larger (∼78 meV) and the increase in intensity observed over the third peak signals that this is due to a combination of the 0–5 transition in the ground state and the 0–1 transition in the $^1\Delta$ state. Nonetheless, the absolute energies and separations of the first three peaks can be used to extrapolate to the energy of the ground state of $NO^-$ and establish an electron affinity of 33±10 meV, which is in good accord with the value from the photodetachment measurements (24+10,−5 meV). The details

of these measurements can be found in Alle *et al.* (1996). They clearly highlight the unique advantages that ToF spectroscopy can provide with the combination of high resolution and high energy accuracy together with the ability to measure absolute cross sections.

### *(3b) Atomic Resonances*

*Triply Excited $He^-$*

Helium, perhaps more than any other system, has been extensively studied with regard to the spectrum of negative ion resonances that it supports. A recent summary of the vast array of experimental studies is provided by Buckman and Clark (1994). It has also attracted substantial theoretical interest and calculations such as ab-initio, multiple-state $R$-matrix approaches have provided a good description of resonance configurations where the two external electrons have principle quantum numbers as high as $n = 5$.

The overwhelming majority of both the experiments and calculations has been concerned with resonances below the first ionisation potential where most of the structure can be considered to be due to doubly excited states (1s $nln'l'$) of the negative ion, in the region of the singly excited spectrum of the neutral atom. However, there has also been a small body of work which has focussed on the region of the spectrum where the helium atom supports many doubly excited (autoionising) states and associated with these states is a spectrum of triply excited negative ion resonances. These resonances have all three electrons excited to the $n = 2$ shell (or higher), resulting in a 'hollow' negative helium ion. These investigations go back to the earliest studies of resonances (e.g. Kuyatt *et al.* 1965), but have also occurred in more recent times (e.g. van der Burgt *et al.* 1986; Batelaan *et al.* 1991). Nonetheless, there remains a number of outstanding questions about these states, which have been highlighted in recent times by the observation of the analogous triply excited states in 'hollow' neutral Li (Diehl *et al.* 1996, 1997).

The present study of these resonances has concentrated on the two lowest lying triply excited resonances, the $2s^2 2p\ ^2P$ and $2s2p^2\ ^2D$ (Fano and Cooper 1965) which occur at $57{\cdot}22$ and $58{\cdot}30$ eV respectively (Hicks *et al.* 1974). It has been conducted on a crossed-beam spectrometer equipped with a position sensitive detector (PSD) at the output of a hemispherical energy analyser. The apparatus was discussed briefly in Section 2. The apparatus is configured to allow the simultaneous measurement of excitation functions for the four $n = 2$ excited states of neutral helium, which have excitation energies of $19{\cdot}82$ eV ($2^3S$), $20{\cdot}62$ eV ($2^1S$), $20{\cdot}96$ eV ($2^3P$) and $21{\cdot}2$ eV ($2^1P$). Measurements were carried out for incident electron energies in the range between 57 and 60 eV, which encompasses the thresholds of the lowest lying doubly-excited, autoionising states of He, the $2s^2\ ^1S$ state at $57{\cdot}8$ eV and the $2s2p\ ^3P$ state at $58{\cdot}1$ eV, and for a range of electron scattering angles between 10° and 120°. As the incident energy is stepped through this range, energy loss spectra are accumulated on the PSD for about 10 seconds per energy. These are then fitted, using a non-linear least squares routine, with a function comprising four gaussians, centred at the spectroscopic energies of each of the four $n = 2$ states. From this fit, which is done at the end of each energy step, the relative DCS for the excitation of each

state is obtained for that energy. This procedure is repeated many times enabling the excitation functions for the four excited states to be measured in this incident energy range. Also measured over the same energy range were a series of elastic scattering 'excitation functions'. Simultaneously with all the scattered electron measurements, excitation functions for the production of metastable ($2^3S+2^1S$) helium atoms were also obtained by measuring the yield of metastable atoms with a channeltron electron multiplier detector. This channel provides a sensitive measure for the position of the two resonances and was used as a routine energy calibration. The apparatus, and the experimental procedure, has been described above and in more detail by Trantham *et al.* (1999).

If the classifications of these states are correct then based on simple angular momentum and parity considerations their decay to the elastic channel, and to the $n = 2$ levels should proceed in the following fashion:

$$
\begin{aligned}
e^- + He(ls^2\,{}^1S) &\Rightarrow He^- 2s^2 2p(^2P) & e^- + He(ls^2\,{}^1S) &\Rightarrow He^- 2s^2 2p(^2D)\\
&\Rightarrow He(1s^2\,{}^1S) + \epsilon p & &\Rightarrow He(1s^2\,{}^1S) + \epsilon d\\
&\Rightarrow He(1s2s\,{}^3S) + \epsilon p & &\Rightarrow He(1s2s\,{}^3S) + \epsilon d\\
&\Rightarrow He(1s2s\,{}^1S) + \epsilon p & &\Rightarrow He(1s2s\,{}^1S) + \epsilon d\\
&\Rightarrow He(1s2p\,{}^3P) + \epsilon s & &\Rightarrow He(1s2p\,{}^3P) + \epsilon p\\
&\Rightarrow He(1s2s\,{}^1P) + \epsilon s & &\Rightarrow He(1s2s\,{}^1P) + \epsilon p.
\end{aligned}
$$

Thus, the first goal of these experiments was to investigate the angular distributions of the autodetached electrons into each final state in order to unambiguously confirm these classifications. The elastic scattering spectra are shown in Fig. 7. At the top of this figure, and in all the other figures in this section, we show the metastable atom excitation function which clearly identifies the two resonances. The remaining three curves represent the elastic excitation function at electron scattering angles of 30°, 54° and 90°, as labelled. It can be clearly seen that at a scattering angle of 30°, both resonances are present in the elastic scattering spectrum. At 54°, the $^2$D feature has vanished, which is consistent with the decay of this resonance to the ground state by autodetachment of a d-wave electron, as predicted in the above guide. Similarly at 90°, the $^2$P resonance has vanished, which again is consistent with the decay scheme oulined above. These results are similar to those obtained many years ago by Hicks *et al.* (1974).

Perhaps of more interest are the spectra shown in Fig. 8. These are excitation functions for the four $n = 2$ states at scattering angles of 16°, 54°, 90° and 105° respectively. At 16°, both of the resonance features are present in the decay to all four excited states, consistent with the decay schemes above, although the decay of the $^2$D state to the $2^{3,1}$P states is very weak. At 54°, both resonances are present in the $2^{3,1}$P states but the $^2$D feature is not evident in either of the $2^{3,1}$S states, which is consistent with the proposed decay to these states by autodetachment of a d-wave electron. At 90° the lowest $^2$P resonance is not evident in either of the $2^{3,1}$S states just as the $^2$D resonance makes no

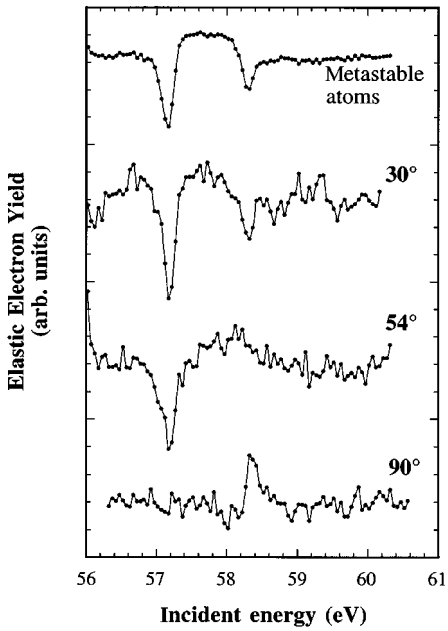


**Fig. 7.** Energy dependence of the elastic electron scattering cross section for helium at angles of 30°, 54° and 90° in the region of the $2s^2 2p\ ^2P$ and $2s2p^2\ ^2D$ resonances. The top spectrum is the metastable atom excitation function (see text).

appearance in the $2^{3,1}P$ states. These observations are consistent with the above scheme which implies an autodetached p-wave electron for both resonance decays to the states mentioned. At 105°, although the energy resolution is noticeably lower, the resonance features are once again evident in all final states. Thus the observed resonance decays are all consistent with what is expected, based on the classifications of Fano and Cooper (1965).

In addition to the decay modes for these two resonances, the present results can also be analysed in order to provide some information regarding their branching ratios into the various final states. For each of the spectra in Fig. 8 we have determined the ratio of the resonant to direct scattering cross sections. Then, with the aid of the theoretical electron impact excitation cross sections for the $n = 2$ states obtained from the convergent close coupling calculation of Fursa and Bray (1997), we have estimated the resonance contribution to each of the

**Table 1. Estimates of the cross section (in units of $10^{-19}$ cm$^2$ sr$^{-1}$) for the decay of the $He^-$ $2s^2 2p\ ^2P$ and $He^-$ $2s2p^2\ ^2D$ resonances to the four $n = 2$ states of helium**

| Angle | $2^3S$ | | $2^1S$ | | $2^3P$ | | $2^1P$ | |
|---|---|---|---|---|---|---|---|---|
| | $^2P$ | $^2D$ | $^2P$ | $^2D$ | $^2P$ | $^2D$ | $^2P$ | $^2D$ |
| 16° | 0·21 | 0·39 | 0·43 | 0·34 | 0·15 | 0·06 | 1·0 | 0·5 |
| 54° | 0·001 | 0 | 0·05 | 0 | 0·20 | 0·06 | 0·16 | 0·03 |
| 90° | 0 | 0·08 | 0 | 0·04 | 0·07 | 0 | 0·06 | 0 |
| 105° | 0·03 | 0·12 | 0·03 | 0·03 | 0·05 | 0·02 | 0·03 | 0·01 |

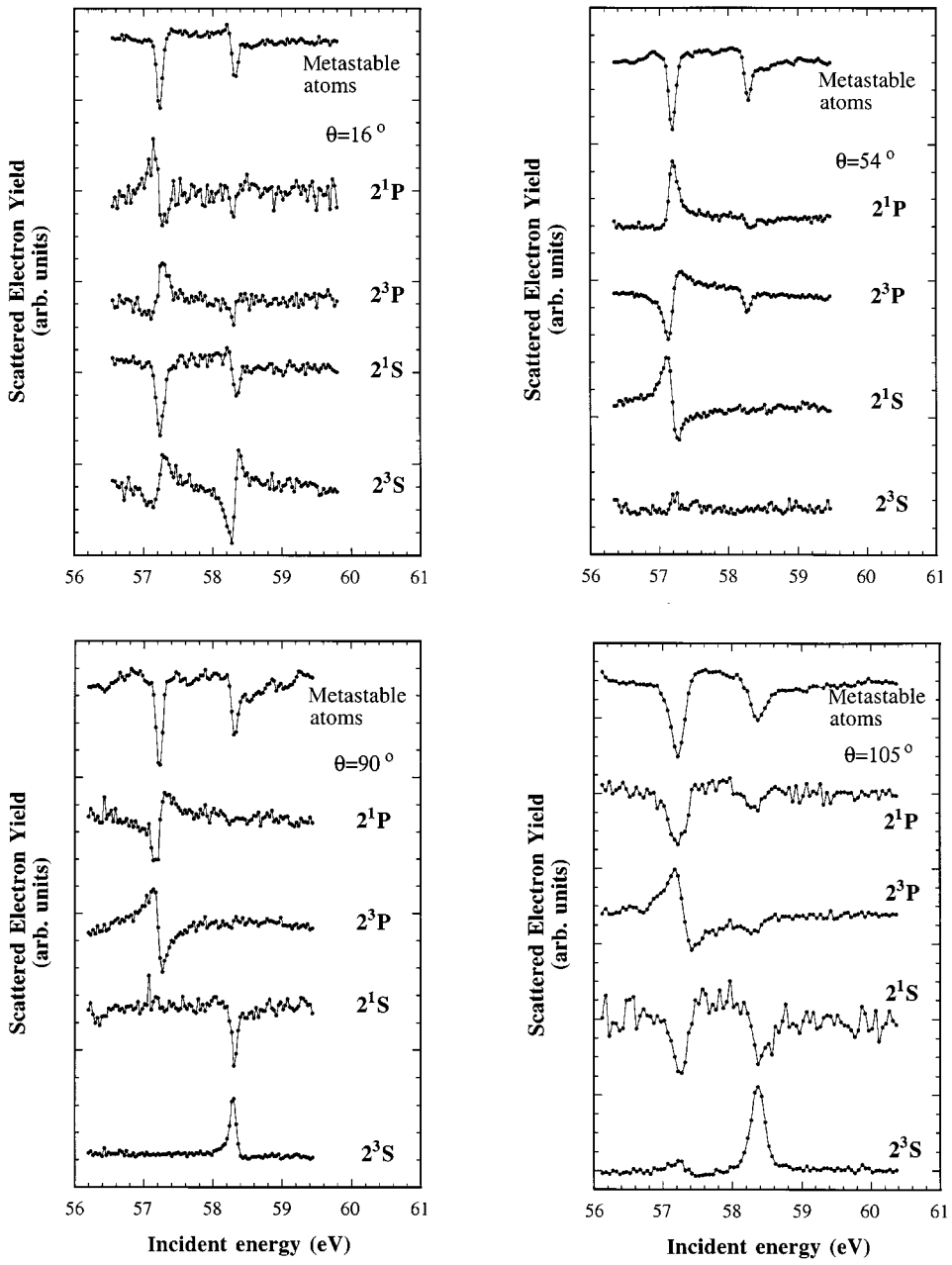


**Fig. 8.** Excitation functions for the $n = 2$ levels of helium at angles of 16°, 54° and 90° and 105° in the region of the $2s^2 2p\ ^2P$ and $2s2p^2\ ^2D$ resonances.

$n = 2$ cross sections for both the $^2P$ and $^2D$ resonances. This procedure assumes that the transmission and detection efficiency of the spectrometer is constant across the energy loss window studied. As the energy loss window is less than 2 eV wide, and the energy of the scattered electrons is greater than 36 eV in all

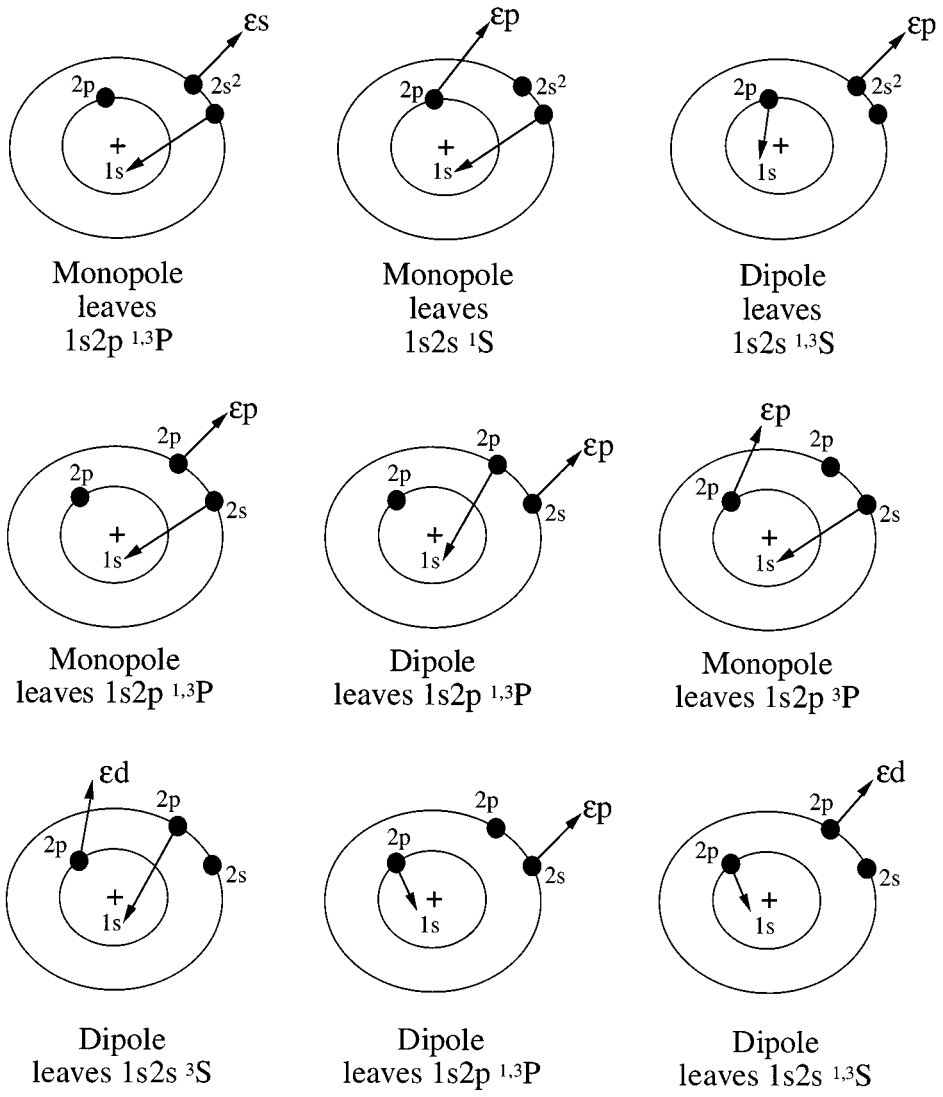


**Fig. 9.** Schematic representation of possible decay modes for the resonances $2s^2 2p\ ^2P$ (top row) and $2s2p^2\ ^2D$ (middle and bottom rows).

cases, this is a reasonable assumption. The resonance cross sections are given in Table 1 and they provide for a number of interesting observations:

- For the $^2P$ resonance, there is apparently no preference in its decay to either of the $2^{1,3}P$ levels. However, in the decay of this resonance to the 2S levels, there is a clear preference, *by about a factor of two* at all angles other than 90° where decay is forbidden, for decay to the $^1S$ over that for the $^3S$.
- For the $^2D$ resonance, at an angle of 54° where decay to either of the $^{1,3}S$ states is forbidden by angular momentum and parity considerations, decay to the $2^3P$ state is favoured over that to the $2^1P$ state *by about a factor of two*

Similarly, at an angle of 90°, where decay to the 2P states is forbidden, decay to the $2^3$S state is once again favoured *by about a factor of two* over that to the $2^1$S state.

We believe that these decay propensities favour a model for these resonances which has two of the electrons in a doubly excited configuration about an excited Coulomb core. We favour this arrangement, over alternatives such as an excited electron weakly bound to a doubly excited neutral state, or three electrons which form an equilateral triangle configuration about the nucleus at centre. In doing so we assume that the observed transitions are primarily autoionisation processes involving a single $1/r_{1,2}$ interaction between two of the three electrons. In expanding this interaction we keep the first two, monopole and dipole, terms. In the monopole, neither electron changes its $l$ value whilst for the dipole term, the two angular Legendre functions result in a simultaneous $\Delta l = 1$ change for both electrons.

In our model the lowest lying $^2$P resonance thus consists of an excited electron pair $(2s^2)^1$S external to an excited $He^+(2p)$ Coulomb core. The possible decay modes are represented schematically in the top row of Fig. 9. Decay to the 1s2p levels can only occur via a monopole transition involving one of the s-electrons being autodetached as $\epsilon$s and the other dropping into the 1s core, with no preference for the two remaining electrons to couple to either $^1$P or $^3$P. This is consistent with the observations in Table 1. On the other hand, decay to the 1s2s levels involves an interaction between the 2p electron and one of the $2s^2$ pair. The monopole decay proceeds via the autodetachment of the 2p electron with one of the 2s electrons dropping into the 1s core resulting in 1s2s $^1$S. The dipole decay involves one of the 2s electrons being autodetached as $\epsilon$p and the 2p electron dropping into the 1s core, the two electrons then coupling to either $^1$S or $^3$S. As the monopole interaction may be expected to dominate, we would expect the decay to the $2^1$S to dominate over that to the $2^3$S and this is consistent with the observations.

For the $^2$D resonance, the energy levels would imply rather unambiguously a resonance configuration $[(2s2p)^3P\ 2p]^2D$. The decay of this resonance can be described by the six diagrams illustrated in the middle and bottom rows of Fig. 9. The 1s2p levels of neutral helium can be populated once again by either monopole or dipole decay. The monopole decay involves a 2s → 1s transition accompanied by the autodetachment of one of the 2p electrons. If it is the 'inner' 2p which departs then the final state must be $1s2p^3P$, whilst if it is the 'outer' then either $^1$P or $^3$P can result. The dipole decay involves a 2p → 1s transition together with the autodetachment of the 2s electron as $\epsilon$p. Regardless of which 2p electron is involved the final state can be either $^1$P or $^3$P. Again, if we assume the monopole process to be the stronger we may expect that the $^2$D resonance will preferentially populate the 1s2p $^3$P state, and this is observed in Table 1, particularly at an angle of 54° where decay of this resonance to the 2s channels is forbidden.

At an angle of 90°, decay of the $^2$D resonance to the 2p states is forbidden and, if the proposed configuration for this resonance of $[(2s2p)^3P\ 2p]^2D$ is correct, then decay to the 2s states can only be realised by dipole processes involving the two 2p electrons. In the first case, the 'outer' 2p electron makes a transition to 1s and the inner departs in an $\epsilon$d channel, leaving the atom in the $1s2s^3$S

state. The second case involves the outer 2p electron detached in an $\epsilon$d channel and the inner 2p $\rightarrow$ 1s, leaving the atom in either the $^1$S or $^3$S state. Again one may expect to see a propensity for the production of 1s2s$^3$S as a result of this resonance decay at this scattering angle and this is consistent with the observations.

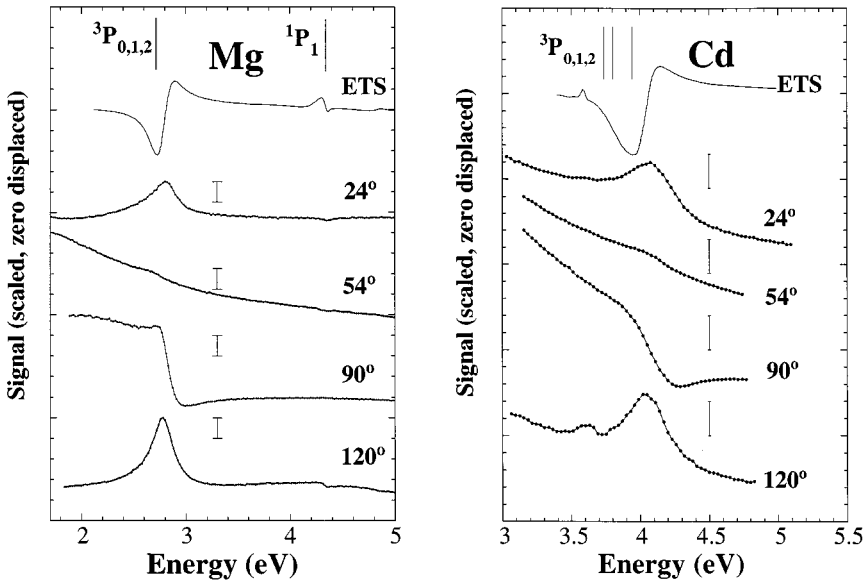


**Fig. 10.** Resonances in the region of the nsnp$^{3,1}$P excited states of Mg and Cd ($n = 3$ and 5 respectively). In each figure the uppermost curve is the electron transmission spectrum (ETS) and the other curves represent elastic electron scattering at the scattering angles indicated. The vertical bars represent 20% of the maximum counts recorded in each spectrum.

*Group II Metals*

The Group II (A and B) metals offer a further opportunity for the study of negative ion resonances formed during electron scattering from two-electron atoms. Furthermore, they also provide the means where the influence of an intermediate shell of d-electrons (in the IIB atoms) on the nature of the negative ion spectrum can be determined.

In the present study we have made a preliminary investigation of the $nsnp^2$ resonances for Mg and Cd, where $n = 3$ and 5 respectively. These resonances, which have been extensively studied in Hg ($n = 6$), straddle in energy the thresholds for the $nsnp^{3,1}$P excited states of these atoms. The present studies have focussed on the complementary benefits of differential elastic electron scattering, electron transmission spectroscopy (ETS) and optical excitation functions.

The configuration $nsnp^2$ will give rise to a large number of possible terms, namely $^2S_{1/2}$, $^2P_{1/2,3/2}$, $^2D_{3/2,5/2}$ and $^4P_{1/2,3/2,5/2}$. All of these features are most clearly manifested in the spectrum of $Hg^-$, where the large spin–orbit interaction and relatively large energy gap between the 6s6p$^3$P$_0$ excited state at 4·67 eV and the first ionisation limit at 10·438 eV, ensure that the resonances

which arise from this configuration are, in the most part, well isolated. Based on the assignments that have been made for these resonances in Hg (see for example Albert *et al.* 1977; Heddle 1975, 1978; Newman *et al.* 1985; Buckman and Clark 1994; Burrow *et al.* 1998) the region near the $^3$P threshold should show resonances due to the $^4P_{1/2,3/2,5/2}$ and $^2D_{3/2,5/2}$ terms. In an environment where the spin–orbit interaction is weak, such as Mg, we may expect that the different spin–orbit terms will be degenerate and that there will be substantial overlap of the resonance features. This appears to be the case in Fig. 10 where we show the results from the elastic scattering and ETS experiments for Mg. A strong, single feature is evident at the threshold of the (essentially degenerate) $3s3p^3P$ levels. Angular momentum and parity considerations imply that of the resonance terms outlined above ($^4P_{1/2,3/2,5/2}$ and $^2D_{3/2,5/2}$), five of the six should decay to the ground state by the autodetachment of a d-wave electron (the final one being s-wave). This is clearly supported by the elastic scattering data which show a minimum in the resonance contribution at an angle of 54°, where the $l = 2$ (d-wave) Legendre polynomial has a minimum. A similar observation can be made for the Cd spectra in Fig. 10. In addition, in Cd, there is evidence in both the ETS and the 120° elastic scattering spectra, of a sharp resonance below the $3s3p^3P$ thresholds. From a comparison with Hg this is most likely due to the $^4P_{1/2}$ term of the $3s3p^2$ configuration.

Perhaps the most striking feature of these resonances, particularly in Mg, is their strong presence in the elastic scattering channel. In Fig. 10 the small vertical bars are intended to indicate the relative contribution of the resonance to the direct elastic scattering cross section. In each part these bars represent 20% of the maximum scattering signal recorded for each spectrum and it can be seen in Mg that scattering via the negative ion accounts for a majority of the elastic scattering signal at several angles.

## 4. Conclusions

Negative ion resonances are ubiquitous in low energy electron scattering from both atoms and molecules. The present work has attempted to summarise a number of negative ion features which have been observed in a range of atomic and molecular targets. In particular, we have focussed on the effect that these states have on low energy electron scattering cross sections and we have attempted to illustrate how scattering measurements can provide substantial insight into the nature of these states. In many cases they provide the most favourable route for the excitation of a particular electronic or vibrational state of an atom or molecule. This is clearly demonstrated, for example, in the present cases of low energy vibrational excitation of $N_2$ and elastic scattering from magnesium. The mechanisms responsible for their formation and decay are also of great interest and they provide a fascinating window on electron correlation effects in the multiple excitation of atomic systems.

## Acknowledgments

It is a pleasure to acknowledge the expertise of Kevin Roberts, Graeme Cornish and Stephen Battisson who have provided technical support for the experiments

outlined here. RJG acknowledges the support of an Australian Research Council Postdoctoral Fellowship. SJB thanks the organisers of the Australian–German Workshop for their support.

## References

Albert, K., Christian, C., Heindorff, T., Reichert, E., and Schön, S. (1977). *J. Phys.* B **10**, 3733.
Allan, M. (1995). *J. Phys.* B **28**, 5163.
Alle, D. T. (1999). PhD Thesis, Australian National University (unpublished).
Alle, D. T., Brennan, M. J., and Buckman, S. J. (1996). *J. Phys.* B **29**, L277.
Batelan, H., van Eck, J., and Heideman, H. G. M. (1991). *J. Phys.* B **24**, 5151.
Birtwistle, D. T., and Herzenberg, A. (1971). *J. Phys.* B **4**, 53.
Boness, M. J. W., and Schulz, G. J. (1970). *Phys. Rev.* A **2**, 2182.
Buckman, S. J., and Clark, C. W. (1994). *Rev. Mod. Phys.* **66**, 539.
Burrow, P. D., Michejda, J. A., Lun, D. R., Sullivan, J. P., McEachran, R. P., Newman, D. S., and Buckman, S. J. (1998). *J. Phys.* B **31**, L1009.
Celotta, R. J., Bennett, R. A., Hall, J. L., Siegel, M. W., and Levine, J. (1972). *Phys. Rev.* A **6**, 631.
Chung, K. T. (1998). *Phys. Rev.* A **58**, 2777.
Diehl, S., *et al*. (1996). *Phys. Rev. Lett.* **76**, 3915.
Diehl, S., *et al*. (1997). *Phys. Rev. Lett.* **79**, 1241.
Ehrhardt, H., and Willmann, K. (1967). *Z. Phys.* **204**, 462.
Fano, U., and Cooper, J. W. (1965). *Phys. Rev.* **138**, 400.
Fursa, D., and Bray, I. (1997). *J. Phys.* B **30**, 757.
Gibson, J. C., Morgan, L. A., Gulley, R. J., Brunger, M. J., Bundschu, C. T., and Buckman, S. J. (1996). *J. Phys.* B **29**, 3197.
Gulley, R. J., Alle, D. T., Brennan, M. J., Brunger, M. J., and Buckman, S. J. (1994). *J. Phys.* B **27**, 2593.
Heddle, D. W. O. (1975). *J. Phys.* B **8**, L33.
Heddle, D. W. O. (1978). *J. Phys.* B **11**, L711.
Herzenberg, A. (1968). *J. Phys.* B **1**, 548.
Hicks, P. J., Cvejanovic, S., Comer, J., Read, F. H., and Sharp, J. M. (1974). *Vacuum* **24**, 573.
Kuyatt, C. E., Simpson, J. A., and Mielczarek, S. R. (1965). *Phys. Rev.* **138**, 385.
Land, J. E., and Raith, W. (1973). *Phys. Rev. Lett.* **30**, 193.
Land, J. E., and Raith, W. (1974). *Phys. Rev.* A **9**, 1592.
Linder, F., and Schmidt, H. (1971). *Z. Naturforsch.* **26a**, 1617.
Morgan, L. A. (1991). *J. Phys.* B **24**, 4649.
Morgan, L. A., and Tennyson, J. (1993). *J. Phys.* B **26**, 2429.
Newman, D. S., Zubek, M., and King, G. C. (1985). *J. Phys.* B **18**, 985.
Sanche, L., and Schulz, G. J. (1972). *Phys. Rev.* A **5**, 1672.
Schulz, G. J. (1973). *Rev. Mod. Phys.* **45**, 378.
Siegel, M. W., Celotta, R. J., Hall, J. L., Levine, J., and Bennett, R. A. (1972). *Phys. Rev.* A **6**, 607.
Srivastava, S. K., Chutjian, A., and Trajmar, S. (1975). *J. Chem. Phys.* **63**, 2659.
Subramanian, K. P., and Kumar V. (1990). *J. Phys.* B **23**, 745.
Sun, W., Morrison, M. A., Isaacs, W. A., Trail, W. K., Alle, D. T., Gulley, R. J., Brennan, M. J., and Buckman, S. J. (1995). *Phys. Rev.* A **52**, 1229.
Sweeney, C. J., and Shyn, T. W. (1997). *Phys. Rev.* A **56**, 1384.
Szmytkowski, C., and Maciag, K. (1996). *Phys. Scripta* **54**, 271.
Trantham, K. T., Jacka, M., Rau, A. R. P., and Buckman, S. J. (1999). *J. Phys.* B **32**, 815.
van der Burgt, P. J. M., van Eck, J., and Heideman, H. G. M. (1986). *J. Phys.* B **19**, 2015.
Weatherford, C. A., and Temkin, A. (1994). *Phys. Rev.* A **49**, 2580.
Zecca, A., Brusa, R. S., Grisenti, R., Oss, S., and Szmytkowski, C. (1986). *J. Phys.* B **19**, 3353.

Manuscript received 19 May, accepted 24 May 1999